Available online at www.sciencedirect.com

ScienceDirect

Mendeleev Commun., 2022, **32**, 742–744

Mendeleev Communications

Comparative structural analysis of a histone-like protein from *Spiroplasma melliferum* in the crystalline state and in solution

Yury A. Gaponov,*[a] Vladimir I. Timofeev,[a,b] Yulia K. Agapova,[a] Eduard V. Bocharov,[c] Eleonora V. Shtykova[b] and Tatiana V. Rakitina[a,c]

[a] *National Research Center 'Kurchatov Institute', 123182 Moscow, Russian Federation. E-mail: gaponov_ya@nrcki.ru*

[b] *A. V. Shubnikov Institute of Crystallography, FSRC 'Crystallography and Photonics', Russian Academy of Sciences, 119333 Moscow, Russian Federation*

[c] *M. M. Shemyakin–Yu. A. Ovchinnikov Institute of Bioorganic Chemistry, Russian Academy of Sciences, 117997 Moscow, Russian Federation*

DOI: 10.1016/j.mencom.2022.11.011

A solution of a histone-like protein from *Spiroplasma melliferum* (HUSpm) was examined by small-angle X-ray scattering (SAXS). The experimental SAXS curve was compared with those calculated for the HUSpm structures from the PDB databank obtained by both X-ray diffraction analysis and nuclear magnetic resonance spectroscopy. The model of the HUSpm structure in solution, which best agrees with the experimental SAXS data, has a shorter distance between the centers of mass of the HUSpm monomers compared to the crystal structure, indicating that the HUSpm monomers can be located closer to each other in solution than in the crystalline state.

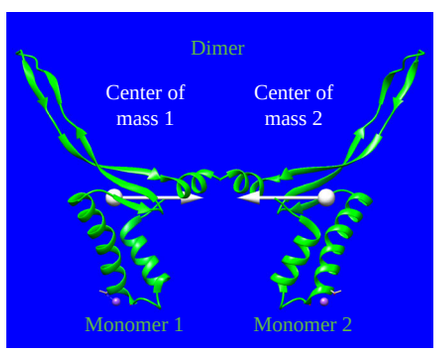

Keywords: small-angle X-ray scattering, SAXS, X-ray diffraction, XRD, nuclear magnetic resonance spectroscopy, NMR, crystal structure, structure in solution, histone-like HU protein.

In general, the shape, size and structure of a protein molecule may differ in the crystalline state and in solution.[1] There are two sources of this difference: structural rearrangements of the molecule during its transition from one state to another and the fact that crystals do not reflect the entire variety of conformations existing in solution.[2] Knowledge of the behavior of macromolecules during the transition from a liquid to a solid state is important from both a theoretical and practical point of view, for example, it is necessary for studying the structure–activity relationship and structure-based drug design.

The histone-like protein HU is the most abundant and ubiquitous nucleoid-associated protein in bacteria.[3,4] This small dimeric protein binds, bents and wraps genomic DNA, playing an important role in nucleoid folding and compaction, as well as in the regulation of major DNA-dependent transactions.[4,5] Despite the well-known involvement of HU in the regulation of viability, adaptability and virulence of pathogenic bacteria,[6,7] only a few chemical inhibitors of the protein with antibacterial activity have been reported until now.[8,9] One of the putative reasons for hindering the successful development of such inhibitors is the mismatch between the crystal structures of HU used for structure-based drug design and protein folding in solution. The aim of this work was to compare the structural characteristics of HU from *Spiroplasma melliferum* (HUSpm) obtained by X-ray diffraction (XRD) analysis and nuclear magnetic resonance (NMR) spectroscopy with those obtained by small-angle X-ray scattering (SAXS).

The implementation of SAXS in combination with NMR spectroscopy and molecular dynamics (MD) simulations is widely used to determine the structure of a protein in solution.[10–12] In such experiments, the SAXS curves calculated for a set of structural models generated by MD simulations, taking into account NMR-derived restraints, are fitted to the experimental SAXS curve. Thus, SAXS data allows reducing the total number of structural models obtained and, consequently, improves the quality of the resulting structures. When the protein under study has flexible parts, the experimental SAXS curve represents the average conformation of the molecule and helps to select the structures closest to this average conformation from the set of MD models of the structure in solution.

Protein samples containing recombinant HUSpm were obtained as previously described.[†,13] Some samples were supplemented with

[†] HUSpm was dissolved in 50 mM sodium phosphate buffer (pH 7.5) with and without DMSO (2.5 vol%) to concentrations of 0.2–0.48 mM. The SAXS experiments were carried out at the P12 beamline (Petra III, Germany) using a beam wavelength λ_b = 1.2 nm.[14] The Pilatus3 X 6M detector system was used as the SAXS image detector. Experimental scattering curves were taken in the range of scattering vectors s = 0.03–7.3 nm^{-1}. A shorter range of scattering vectors was used for calculations. SAXS data collection for protein samples was performed 20 times; for all protein samples, buffer data collection was performed before and after sample data collection. All experimental SAXS data were processed by the ATSAS software suite.[15]

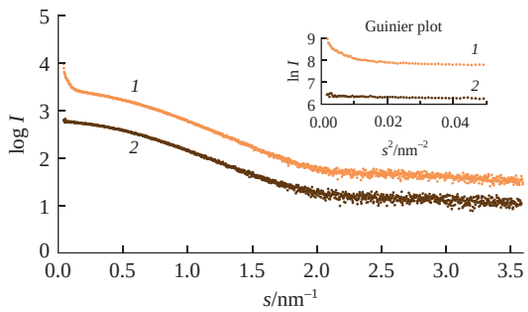

Figure 1 Comparison of SAXS curves obtained for samples containing (*1*) 0.48 mM HUSpm and (*2*) 0.2 mM HUSpm + DMSO. The inset shows the Guinier plot of the onset of the SAXS curves.

DMSO, which is the commonly used organic solvent. The HUSpm solution was studied by the SAXS method using a synchrotron X-ray source.† The SAXS curves, with the exception of the curve obtained for a 0.2 mM protein solution in the presence of DMSO, demonstrate a significant increase in the scattering intensity in the region of small values of the scattering vector (s = 0–0.2 nm^{-1}), which indicates the aggregation of molecules (Figure 1). The SAXS curve of the sample containing DMSO and HUSpm at 0.2 mM demonstrates the best quality (no aggregation) and was chosen for further analysis.

Both the crystal structure of HUSpm (PDB ID 5L8Z) obtained by XRD analysis[13] and 15 models of the structure of HUSpm in solution (PDB ID 5OGU) created by the MD simulation based on NMR-derived distance and dihedral constraints[16] were used to construct a set of calculated SAXS curves, which were fitted to the experimental SAXS curve using the CRYSOL3 software.[15]

Table 1 shows the results of fitting. According to the published work,[12] the goodness of the fit was assessed by the values of the reduced chi-square (χ^2_v) and the Guinier radius (R_g): both the decrease in the value of the reduced χ^2_v and the closeness of the R_g value to the experimental one indicate a better fit of the calculated SAXS curve to the experimental one. Since the dimer is the functional unit of any HU protein, we also evaluated the relative position of the monomers in the HUSpm homodimer by calculating the distance D_{mon} between the centers of mass of the HUSpm monomers (Figure 2). D_{mon} is defined by equation (1):

$$D_{mon} = \sqrt{(C_{1,x} - C_{2,x})^2 + (C_{1,y} - C_{2,y})^2 + (C_{1,z} - C_{2,z})^2}, \quad (1)$$

where $C_{1,x}$, $C_{1,y}$, $C_{1,z}$, $C_{2,x}$, $C_{2,y}$, $C_{2,z}$ are the x, y, z coordinates of the centers of mass of the monomers, which, in turn, were calculated using equation (*2*):

$$C_{mon} = \frac{\sum_i r_i m_i}{M}, \quad (2)$$

where r_i and m_i are the coordinates and mass of the i^{th} atom of the monomer, respectively, and M is the mass of the monomer molecule. In the PDB-deposited structures, the atomic coordinates have three decimal places. The relative error in calculating the value of D_{mon} is about $(\delta D_{mon})/D_{mon} \leqslant 0.01$.

According to Table 1, in all cases, the R_g values confirm the dimeric structure of HUSpm. It should be noted that the 15 models generated for the HUSpm structure 5OGU in solution can be sorted into two clusters and a single cluster model. All structures from the 1st cluster and the corresponding average structure have smaller values of χ^2_v and R_g values closer to the experimental value compared to those from the 2nd cluster and the single cluster model (see Table 1). Thus, we can conclude that the structures from the 1st cluster are in better agreement with the SAXS results. All structures from the 1st cluster have smaller values of R_g and D_{mon} than the structures from the 2nd cluster.

Table 1 Goodness parameters for fitting the calculated SAXS curves to the experimental one and the distance between the centers of mass of the HUSpm monomers for the PDB-retrieved HUSpm structures in solution (PDB ID 5OGU) and in the crystalline state (PDB ID 5L8Z), as well as for the experimental HUSpm structure in solution.

PDB ID	Model no.	χ^2_v	R_g/nm	D_{mon}/nm
5OGU	1st cluster of models for the NMR-derived structure in solution			
	1	1.42	2.08	0.74
	2	1.28	2.12	0.67
	3	1.54	2.08	0.64
	4	1.61	2.07	0.69
	5	1.38	2.11	0.75
	6	1.43	2.10	0.68
	7	1.41	2.10	0.62
	Average	1.44 ± 0.1	2.09 ± 0.02	0.68 ± 0.05
	2nd cluster of models for the NMR-derived structure in solution			
	8	1.84	2.19	0.80
	9	2.54	2.28	0.91
	10	3.00	2.31	0.98
	11	2.72	2.29	0.89
	12	2.95	2.29	0.88
	13	2.78	2.27	0.90
	14	2.78	2.26	0.90
	Average	2.66 ± 0.4	2.27 ± 0.04	0.89 ± 0.05
	Single model for the NMR-derived structure in solution			
	15	2.00	2.22	0.86 ± 0.01
5L8Z	Crystal structure by XRD analysis			
	–	1.36	2.19	0.75 ± 0.01
–	Experimental SAXS curve			
	–		2.14 ± 0.05	

According to the lowest χ^2_v value (1.28) and the R_g value (2.12 nm), which is closest to the experimental one (2.14 nm), model 2 from the 1st cluster demonstrates a better fit to the experimental SAXS curve than to the curve calculated for the HUSpm crystal structure 5L8Z (see Table 1 and Figure 3). However, the R_g value of the crystal structure (2.19 nm) also corresponds to this parameter of the experimental SAXS curve within the experimental error. Given the high flexibility of the HUSpm DNA-binding domain (see Figure 3, inset), we can conclude that model 2 from the 1st cluster provides the best representation of the average conformation of the HUSpm dimer in solution. It should be noted that model 2 has a smaller D_{mon} value (0.67 nm) compared to that calculated for the HUSpm crystal structure (0.75 nm), although the difference between the above D_{mon} values (0.08 ± 0.01 nm) is very small. Nevertheless, the result might serve as an indication that in solution the HUSpm monomers can

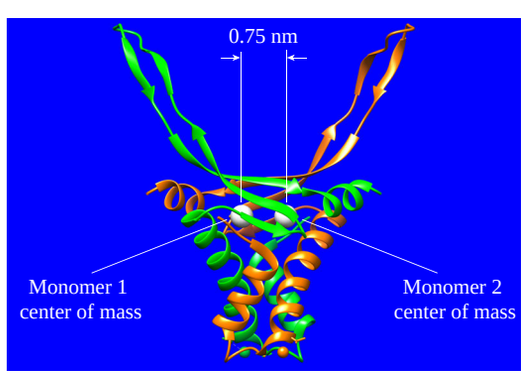

Figure 2 Location of the centers of mass in the HUSpm dimer. The HUSpm crystal structure (PDB ID 5L8Z) is shown as a ribbon diagram. Different monomers are colored gold and green, and their centers of mass are marked with white balls. The drawing was created using the UCSF Chimera software.[17]

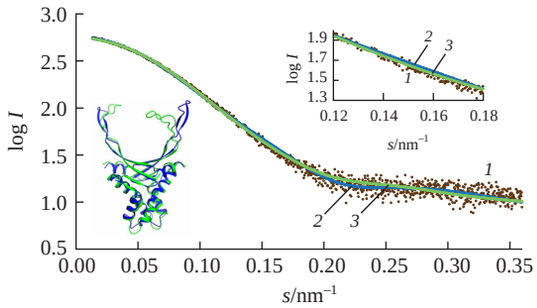

Figure 3 Comparison of (*1*) the experimental SAXS curve with the curves calculated for the HUSpm structures (*2*) in the crystalline state (PDB ID 5L8Z) and (*3*) in solution (according to best fitted model 2 from the 1st cluster generated from the PDB ID 5OGU structure in solution). The inset in the upper right corner shows the expanded area of the curves. The inset in the lower left corner shows the Cα-atom superposition of the crystal structure 5L8Z (blue) and the structure according to model 2 from the 1st cluster for the HUSpm structure 5OGU in solution (green). Superposition was performed using the PyMol software[20] with a standard deviation of 0.13 nm.

be located closer to each other than in the crystalline state of the protein. It is known[18,19] that macromolecules in solution are surrounded by a shell of solvent molecules with a thickness of about 0.3–0.5 nm, which could be the putative reason for the displacement of HUSpm monomers towards each other.

In conclusion, the SAXS experiment and a comparative analysis of the structures of the HUSpm dimer in solution and in the crystalline state were carried out. The obtained experimental SAXS curve was compared with those calculated for the HUSpm crystal structure (PDB ID 5L8Z) and for 15 models of the HUSpm structure in solution (PDB ID 5OGU). It has been shown that only half of the MD models of the HUSpm structure in solution fit the experimental SAXS curve well, and of these, one model fits the experimental data better than the high-resolution crystal structure, indicating the advantage of using the SAXS experiment for structural filtering and validation of MD models of the protein structure in solution.

This work was supported by the Russian Foundation for Basic Research (project no. 20-04-01001) in part of data acquisition and analysis in the SAXS experiment. We acknowledge the Ministry of Science and Higher Education of the Russian Federation (State Assignment for the FSRC ‘Crystallography and Photonics’ of RAS) and NRC ‘Kurchatov Institute’ (order no. 2557 dated 28.10.2021) for partial support of the structural analysis.

References

1 S. Keiffer, M. G. Carneiro, J. Hollander, M. Kobayashi, D. Pogoryelev, E. Ab, S. Theisgen, G. Müller and G. Siegal, *J. Biomol. NMR*, 2020, **74**, 521.
2 A. Carlon, E. Ravera, W. Andrałojć, G. Parigi, G. N. Murshudov and C. Luchinat, *Prog. Nucl. Magn. Reson. Spectrosc.*, 2016, **92**–**93**, 54.
3 A. Grove, *Curr. Issues Mol. Biol.*, 2011, **13**, 1.
4 D. Kamashev, Y. Agapova, S. Rastorguev, A. A. Talyzina, K. M. Boyko, D. A. Korzhenevskiy, A. Vlaskina, R. Vasilov, V. I. Timofeev and T. V. Rakitina, *PLoS One*, 2017, **12**, e0188037.
5 R. T. Dame, F.-Z. M. Rashid and D. C. Grainger, *Nat. Rev. Genet.*, 2020, **21**, 227.
6 P. Stojkova, P. Spidlova and J. Stulik, *Front. Cell Infect. Microbiol.*, 2019, **9**, 159.
7 J. Hołówka and J. Zakrzewska-Czerwińska, *Frontiers in Microbiology*, 2020, **11**, 590.
8 T. Bhowmick, S. Ghosh, K. Dixit, V. Ganesan, U. A. Ramagopal, D. Dey, S. P. Sarma, S. Ramakumar and V. Nagaraja, *Nat. Commun.*, 2014, **5**, 4124.
9 Y. K. Agapova, D. A. Altukhov, V. I. Timofeev, V. S. Stroylov, V. S. Mityanov, D. A. Korzhenevskiy, A. V. Vlaskina, E. V. Smirnova, E. V. Bocharov and T. V. Rakitina, *Sci. Rep.*, 2020, **10**, 15128.
10 P. Rodríguez-Zamora, *Prog. Biophys. Mol. Biol.*, 2020, **150**, 140.
11 T. Bengtsen, V. L. Holm, L. R. Kjølbye, S. R. Midtgaard, N. T. Johansen, G. Tesei, S. Bottaro, B. Schiøtt, L. Arleth and K. Lindorff-Larsen, *eLife*, 2020, **9**, e56518.
12 A. H. Larsen, Y. Wang, S. Bottaro, S. Grudinin, L. Arleth and K. Lindorff-Larsen, *PLoS Comput. Biol.*, 2020, **16**, e1007870.
13 K. M. Boyko, T. V. Rakitina, D. A. Korzhenevskiy, A. V. Vlaskina, Y. K. Agapova, D. E. Kamashev, S. Y. Kleymenov and V. O. Popov, *Sci. Rep.*, 2016, **6**, 36366.
14 C. E. Blanchet, A. Spilotros, F. Schwemmer, M. A. Graewert, A. Kikhney, C. M. Jeffries, D. Franke, D. Mark, R. Zengerle, F. Cipriani, S. Fiedler, M. Roessle and D. I. Svergun, *J. Appl. Crystallogr.*, 2015, **48**, 431.
15 K. Manalastas-Cantos, P. V. Konarev, N. R. Hajizadeh, A. G. Kikhney, M. V. Petoukhov, D. S. Molodenskiy, A. Panjkovich, H. D. T. Mertens, A. Gruzinov, C. Borges, C. M. Jeffries, D. I. Svergun and D. Franke, *J. Appl. Crystallogr.*, 2021, **54**, 343.
16 V. I. Timofeev, D. A. Altukhov, A. A. Talyzina, Y. K. Agapova, A. V. Vlaskina, D. A. Korzhenevskiy, S. Yu. Kleymenov, E. V. Bocharov and T. V. Rakitina, *J. Biomol. Struct. Dyn.*, 2018, **36**, 4392.
17 E. F. Pettersen, T. D. Goddard, C. C. Huang, G. S. Couch, D. M. Greenblatt, E. C. Meng and T. E. Ferrin, *J. Comput. Chem.*, 2004, **25**, 1605.
18 F. Persson, P. Söderhjelm and B. Halle, *J. Chem. Phys.*, 2018, **148**, 215101.
19 S.-Y. Sheu and D.-Y. Yang, *J. Phys. Chem. B*, 2010, **114**, 16558.
20 L. Schrödinger and W. DeLano, *PyMOL*, 2020, https://www.pymol.org/pymol.html.

Received: 21st April 2022; Com. 22/6876